Weierstraß-Institut

für Angewandte Analysis und Stochastik

Leibniz-Institut im Forschungsverbund Berlin e. V.

Preprint ISSN 0946 – 8633

Multi-channel wavelength conversion using four-wave mixing in semiconductor ring lasers

Antonio Pérez-Serrano[1], Julien Javaloyes[2] , Salvador Balle[3]

submitted: August 30, 2012

[1] Weierstrass Institute
Mohrenstr. 39
10117 Berlin
Germany
E-Mail: Antonio.Perez-Serrano@wias-berlin.de

[2] Universitat de les Illes Balears
Cra. Valldemossa, km 7.5
07122 Palma de Mallorca
Spain
E-Mail: julien.javaloyes@uib.es

[3] Institut Mediterrani d'Estudis Avançats
C/ Miquel Marquès 21
07190 Esporles
Spain
E-Mail: salvador@imedea.uib-csic.es

No. 1728
Berlin 2012

2010 *Mathematics Subject Classification.* 78A60, 65P99.

2010 *Physics and Astronomy Classification Scheme.* 42.55.Px, 42.65.Hw, 42.65.Sf.

Key words and phrases. Semiconductor lasers, semiconductor ring lasers (SRLs), four-wave mixing (FWM), all-optical wavelength conversion, travelling wave model (TWM).

J. Javaloyes and S. Balle acknowledge financial support from the Ramón y Cajal program and from project ALAS (TEC2009-14581-C02-01).

Edited by
Weierstraß-Institut für Angewandte Analysis und Stochastik (WIAS)
Leibniz-Institut im Forschungsverbund Berlin e. V.
Mohrenstraße 39
10117 Berlin
Germany

Fax: +49 30 20372-303
E-Mail: preprint@wias-berlin.de
World Wide Web: http://www.wias-berlin.de/

Abstract

We theoretically study all-optical simultaneous wavelength conversion of multiple channels by four-wave mixing in semiconductor ring lasers. Locking the semiconductor ring laser to a holding beam allows to achieve large conversion efficiencies with good signal-to-noise ratio in several channels at multi-Gb/s bit rates. Cross-talk between signals, arising from the peculiar four-wave mixing cascade of modes in semiconductor ring lasers and their cross-gain saturation, is studied in detail. We show that it can be controlled by adjusting the intensity of the holding beam, the bias current of the laser and the number, intensity and wavelength of signals that one wants to convert.

1 Introduction

All-optical multi-channel wavelength converters allow to enhance the capacity and flexibility of future all-optical networks based on Wavelength-Division-Multiplexing (WDM). The possible candidates to perform this task should have the following properties: (a) transparency to the modulation format and speed of the incoming signal and the capacity to reuse the signal for further processing; (b) high integrability with other components such as laser sources and filters in Photonic Integrated Circuits (PICs); and (c) simultaneous and asynchronous conversion of more than one signal. Numerous approaches have been demonstrated mainly based on the use of non-linear effects such as Cross-Gain Modulation (XGM), Cross-Phase Modulation (XPM) or Four-Wave Mixing (FWM) in Semiconductor Optical Amplifiers (SOAs) [1]. Here, the incoming data signal on one particular channel is replicated onto one or several (multicast) channels by coupling it to one or several Continuous Wave (CW) sources. Recently, the concept of FWM-SOA-based converters has been extended to perform simultaneous conversion of different incoming signals reaching rates of 10 Gb/s [2] and even higher bit rates (50 Gb/s) have been achieved by using quantum-dot SOAs [3]. However it should be noticed that SOA-based approaches have a high power consumption due to the high bias current needed in the SOA and the bias currents needed to generate the CW beams.

Semiconductor Ring Lasers (SRLs) are highly integrable devices that have shown their potential for performing all-optical processing while having a low power consumption. Applications such as all-optical memory [4] and data processing [5] have been demonstrated exploiting the directional emission bistability exhibited by SRLs [6]. Furthermore, SRLs have shown cavity-enhanced FWM [7] that provides rich opportunities for implementing THz radiation generators, logical gates [8] and wavelength converters [9].

In this paper, we propose exploiting the FWM properties of SRLs for simultaneous wavelength conversion of multiple channels. We investigate numerically the dynamics of the SRL via a semi-classical Travelling Wave Model (TWM) [10] that allows us to naturally describe spatial effects and multi-mode operation in time-scales longer than 1 ps. The model is tested against the experimental results reported in [7] and [9], and then applied to analyze simultaneous multi-channel wavelength conversion. We discuss the impact of cross-talk effects and possible mitigation strategies.

2 The model

We summarize here the TWM developed in [10] for the slowly varying amplitudes of the clockwise and counter-clockwise fields, $E_{\pm}(z,t)$. We assume a single-transverse mode waveguide that supports a single TE mode of optical frequency ω_0. We take the effect of the presence of counter-propagating fields explicitly into account expressing the carrier density as $N(z,t) = N_0(z,t) + N_{+2}(z,t)e^{2iq_0z} + N_{-2}(z,t)e^{-2iq_0z}$, where $q_0 = n_g\omega_0/c$, n_g is the group refractive index, N_0 is the local average of the carrier density and $N_{+2}(z,t) = N^*_{-2}(z,t)$ describes the amplitude of the carrier spatial modulation at half the optical wavelength, it describes the Spatial Hole Burning. Scaling space and time to the ring length L_r and the ring transit time $\tau_r = n_gL_r/c$, our TWM reads

$$(\partial_t \pm \partial_z)E_{\pm} = iP_{\pm} - \alpha_i E_{\pm}, \tag{1}$$

$$\partial_t N_0 = J - R(N_0) - i(P_+E_+^* + P_-E_-^* - c.c.), \tag{2}$$

$$\partial_t N_{\pm 2} = -[R'(N_0) + \eta]N_{\pm 2} - i(P_{\pm}E_{\mp}^* - E_{\pm}P_{\mp}^*), \tag{3}$$

where $P_{\pm}(z,t)$ are the medium polarizations, α_i are the internal losses, J is the injected current density, $R(N) = AN + BN^2 + CN^3$ takes into account the carrier recombination, with A, B and C being the non radiative, bi-molecular and Auger recombination coefficients, respectively; $R' = dR/dN$ is the effective interband carrier relaxation rate and $\eta = 4\mathcal{D}q_0^2$ where $\mathcal{D}$ is the ambipolar diffusion coefficient.
The polarizations of the medium, $P_{\pm}(z,t)$, are determined from a mesoscopic approximation to the optical response of the semiconductor quantum well (QW) material [11] and computed via a convolution integral [12]

$$\begin{aligned} P_{\pm}(z,t) = \textstyle\int_0^\infty dt' \, \{\chi[t', N_0(z,r)]E_{\pm}(z,r) \\ +\chi_N[t', N_0(z,r)]N_{\pm 2}(z,r)]E_{\mp}(z,r)\} + \beta\xi_{\pm}(z,t), \end{aligned} \tag{4}$$

where $r = t - t'$ and the convolution kernel $\chi = \chi[t', N(z,r)]$ and its variation with carrier density, $\chi_N = \partial\chi/\partial N$, can be found in [12]. We also add spontaneous emission of amplitude β by including a Gaussian white noise term $\xi_{\pm}(z,t)$ of zero mean and correlation $\langle\xi_{\pm}(z,t)\xi_{\pm}(\hat{z},\hat{t})\rangle = \delta(t-\hat{t})\delta(z-\hat{z})$,
The TWM defined by Eqs. (1)-(4) has to be closed with the boundary conditions for the ring cavity, that read

$$\begin{aligned} E_+(0,t) = t_+E_+(1,t) + r_-E_-(0,t) + \sum_m Y_m^+(t)e^{-i\omega_m t}, \\ E_-(1,t) = t_-E_-(0,t) + r_+E_+(1,t) + \sum_m Y_m^-(t)e^{-i\omega_m t}, \end{aligned} \tag{5}$$

where $t_{\pm}$ and $r_{\pm}$ are the transmission and reflection coefficients at the output coupler for the $E_{\pm}$ fields respectively, and the injected signals at each mode m in each propagation direction are $Y_m^{\pm}(t)$, respectively. In the following section we use either constant injections fields with smooth rising and falling edges or NRZ signals having a flat top and $\arctan$ shape for rise and fall times of 5 ps.

The parameter set used in this paper is given in Table 1. Numerical integration of the TWM is performed after recasting it into an ensemble of Delayed Algebraic Equations (DAEs) [13] using a spatial discretization of $N = 1201$ points (corresponding to a time step $\Delta t = 10.4$ fs) with a decimation factor $D = 30$; the convolution kernels are computed using $M = 36$ in the past.

Table 1: Model parameters

Symbol	Value	Units	Meaning
Waveguide Parameters			
ω_0	340	THz	Emission frequency
n_g	3.6	-	Effective group index
τ_r	12.5	ps	Ring transit time
L_r	1.04	mm	Length of the ring cavity
$2\alpha_i$	14.4	cm^{-1}	Internal losses
$t_{\pm}$	0.8	-	Transmission coefficients
$r_{\pm}$	1×10^{-4}	-	Reflection coefficients
Active Material Parameters			
N_t	1×10^{18}	cm^{-3}	Transparency carrier density
$\mathcal{D}$	36	cm^{2}s^{-1}	Ambipolar diffusion coefficient
A	1×10^{-8}	s^{-1}	Non radiative recombination
B	7×10^{-10}	cm^{3}s^{-1}	Spontaneous recombination
C	1×10^{-29}	cm^{6}s^{-1}	Auger recombination
$2\chi_0$	86.76	cm^{-1}	Maximum modal gain
γ	16×10^{12}	rad s^{-1}	Polarization decay rate
Ω_T	25×10^{13}	rad s^{-1}	Top of the band frequency
β	1×10^{-5}	-	Spontaneous emission

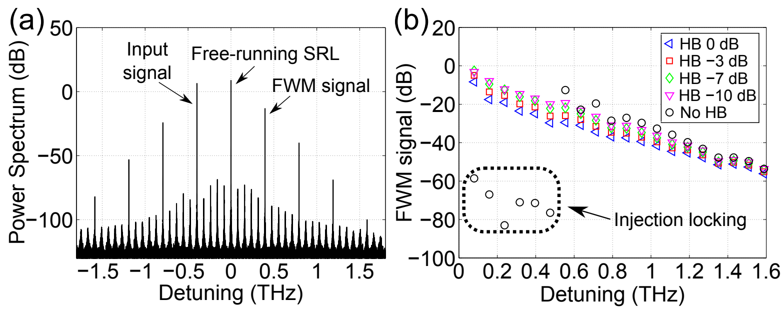

Figure 1: (a) Power spectrum for the E_+ field. The initial state was a clockwise state with an intensity of 17 dB, the co-propagating constant input signal has -20 dB at $m = -5$ (-390 GHz) and produces a cascade of FWM signals. Note how the injection is enhanced by the cavity quality factor to reach $+10$ dB hence amplifying the FWM effects. $J = 5J_{th}$. (b) Intensity of the FWM signal versus the detuning with respect to the free-running SRL mode for different HB intensity values. $J = 5J_{th}$. Without a HB and for small detuning, the injection frequency is locked; while using a HB, high FWM signal values are obtained for small detuning. Note that the discrete points of the detuning are given by the SRL cavity modes.

3 Results and discussion

3.1 One channel conversion and multicast

Biasing the SRL in the unidirectional regime and injecting a light beam in the co-propagating direction of emission of the SRL at a wavelength detuned from the lasing mode produces a cascade of modes as consequence of the FWM in agreement with experiments [7]. This situation is depicted in Fig. 1 (a), where the SRL is biased at $J = 5J_{th}$, the initial state is a E_+ field with an intensity of 17 dB, and a CW beam of intensity -20 dB is injected at mode $m = -5$ (detuning of -390 GHz): as a consequence of the injection, a cascade of modes appear at $m = 5$, $m = \pm 10$, $m = \pm 15$ and $m = \pm 20$, being $m = 5$ the one with higher intensity indicated as the FWM signal.

This process, then, would allow for multicast conversion of an input signal. However, problems may arise due to e.g. locking at the injected wavelength if the intensity of the injected signal is high enough or if directional switching via non-linear processes occurs [14]. In the case depicted in Fig. 1 (b), injection locking of the SRL occurs over the first six modes for injection intensities of -20 dB, and no FWM is obtained in this range.

These problems can be overcome using a CW Holding Beam (HB) to lock the SRL frequency. In these conditions, high FWM intensities can be obtained even for small detuning values. This is shown in Fig. 1 (b), where we plot the intensity of the FWM signal versus the detuning of signal beams of -20 dB amplitude located on the red side of the HB. As the intensity of the HB increases, the FWM signal is reduced due to gain saturation of the medium by the HB and the injected signal, but this can be compensated by increasing the bias current in the SRL. The behaviour is qualitatively the same for positive detunings, although in this case the intensity of the FWM signal can increase using the HB due to the non-symmetrical shape of the semiconductor

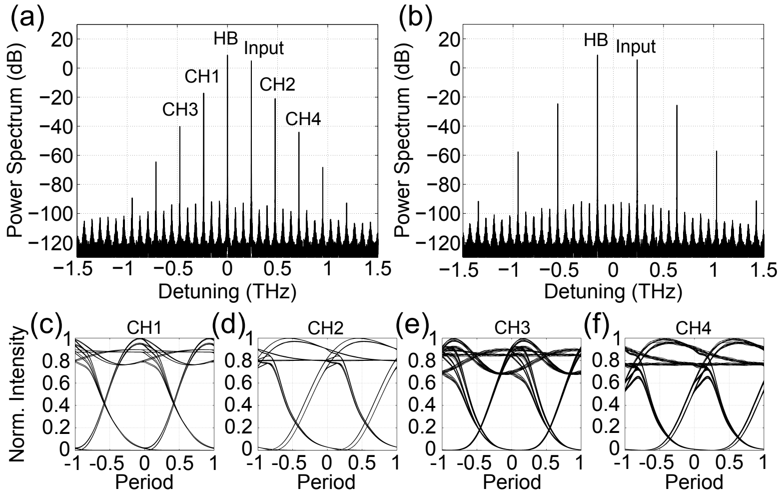

Figure 2: AOM. (a) Power spectrum with an input signal at $m = 3$ (240 GHz) with an intensity of -10 dB and a HB at 0 detuning with an intensity of 0 dB. Four output channels are indicated as CH1 ($m = -3$,-240 GHz) , CH2 ($m = 6$, 475 GHz), CH3 ($m = -6$,-475 GHz) and CH4 ($m = 9$, 710 GHz). (b) Reconfigured AOM. The input signal is the same as in (a), but the HB is injected at $m = -2$ and the converted output signals appear at different modes. (c), (d), (e) and (f) Eye diagrams for the output channels corresponding to (a). The input NRZ signal at 2.5 Gb/s has an intensity of -10 dB.

gain curve, which leads to optical pumping of the medium for large enough detuning.

This approach was used in [9] to demonstrate All-Optical Multicast (AOM) exploiting the cascade of modes obtained via FWM in SRLs while injecting a HB. The TWM successfully reproduces this experiment. Fig. 2 (a) shows the AOM power spectrum for an input signal at $m = 3$ with an intensity of -10 dB and a HB at 0 detuning with an intensity of 0 dB. The input signal is modulated NRZ at 2.5 Gb/s, and the eye diagrams of the converted channels (see Figs. 2 (c-f)) are clearly open. The AOM channels can be modified by changing the wavelength of the HB, as shown in Fig. 2 (b), where the input signal is the same as in the previous case, but the HB is now at $m = -2$.

3.2 Simultaneous multi-channel conversion

The enhanced FWM efficiency due to the cavity resonances of the SRL can be exploited also for simultaneous wavelength conversion of different input signals. In this situation, however, the FWM cascade phenomenon can pose a problem because it can induce strong cross-talk effects, but they can be minimized by choosing the proper injection frequencies or modes. The injection has to be performed in non-multiple modes in order to avoid cross-talk as much as possible. The amount of cross-talk also depends on the number of signals that one wants to simultaneously convert, because the multiple combinations between injected signals have also to be avoided. For example, to convert two signals one can use $m = \pm 2$ and $m = \pm 3$, or $m = \pm 2$ and $m = \pm 5$, to convert three signal one can use $m = \pm 3$, $m = \pm 5$ and $m = \pm 7$, or $m = \pm 5$, $m = \pm 7$ and $m = \pm 11$, and so on. The situation is illustrated in Fig. 3. Panel (a) shows

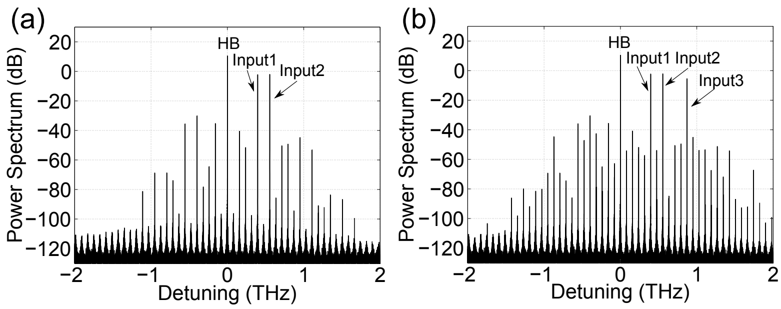

Figure 3: Simultaneous input of various constant fields while injecting a HB at zero detuning with an intensity of 0 dB. (a) Inputs at $m = 5$ (395 GHz) and $m = 7$ (550 GHz) with an intensity of -10 dB. (b) Inputs at $m = 5$, $m = 7$ and $m = 11$ (870 GHz) with an intensity of -10 dB.

the power spectrum when a HB of 0 dB intensity is injected at $m = 0$ and two constant fields with an intensity of -10 dB are injected at $m = 5$ and $m = 7$, respectively. A large number of modes become excited via direct and secondary FWM, but spectral regions where no FWM products develop are clearly seen as e.g. around $m = \pm 11$. These windows can be used to inject another input signal that will also be converted while leaving the other channels almost the same, as shown in panel (b) shows the same situation as (a) after adding a constant field of -10 dB at $m = 11$. The addition of this field triggers an additional cascade of FWM processes, but the FWM products of the original fields (i.e. $m = -5$ and $m = -7$) remain mostly unaffected. This configuration can be thus used to convert three input NRZ signals simultaneously, as show in Fig. 4. In the case considered, all the input signals have -10 dB intensity, the signal at mode $m = 5$ has a bit rate of 5 Gb/s, and the signals at modes $m = 7$ and $m = 11$ have a bit rate of 2.5 Gb/s (see time traces in Fig. 4 (a)). The time traces of the converted signals are determined by filtering the output of the SRL (see Fig. 4 (b)) and used to construct the corresponding eye diagrams in Figs. 4 (c-e). The converted signals accurately reproduce the original signals with a high Optical Signal-to-Noise Ratio that allows amplifying the signals in case their intensity is too low. Cross-talk effects appear via cross-gain saturation of the carriers, and they manifest as variations of the high-level achieved in the converted signals. Moreover, they lead to spikes and/or deformation of the converted signals when one channel is turned on or off, which together with the carrier recovery time can pose problems for operation at high bit rates. The maximum achievable bit rate can be estimated as twice the differential carrier recombination rate, $\sim 2R'(N)$. In Fig. 4, $R'(N_{th}) = 2.5$ GHz, hence reliable conversion can be obtained up to bit rates of 5 Gb/s (see Fig. 4 (c)).

Cross-talk between signals depends on the bias current and the intensity of the HB and signal beams, non-linearly mediated by the semiconductor medium. The cross-talk can be reduced by increasing the intensity of the HB at the price of reducing the intensity of the FWM signals, as show in Fig. 1 (b), and a compromise between the intensity and quality of the output FWM signals has to be found by adjusting the intensities of the injected fields and the density current of the SRL.

One theoretically possible approach to diminish cross-talk effects is to simultaneously inject into the SRL the signals and their negated replicae in counter-propagating directions. Fig. 5(a-c) show the eye diagrams of three converted signals at modes $m = -3, -5$ and -7, respectively,

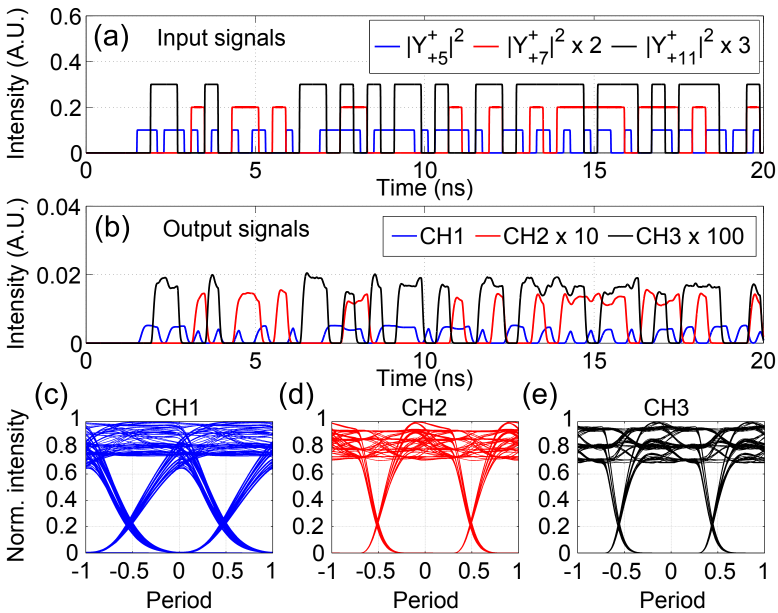

Figure 4: Simultaneous multi-channel conversion while injecting a HB at zero detuning with an intensity of 0 dB. (a) Time trace of the input NRZ signals at modes $m = 5, 7$ and 11. The signal at $m = 5$ has a bit rate of 5 Gb/s while the other signals have a bit rate of 2.5 Gb/s. The intensity of all the signals is the same, -10 dB. (b) Time traces of the converted signals at modes $m = -5, -7$ and -11, denoted as CH1, CH2 and CH3 respectively. (c), (d) and (e) eye diagrams of the converted signals.

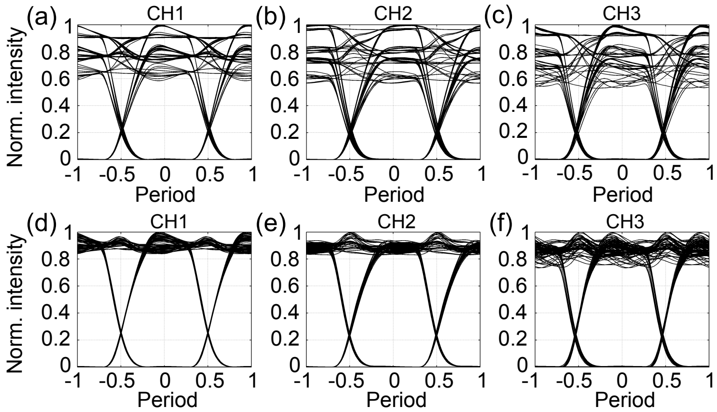

Figure 5: Simultaneous multi-channel conversion of three 2.5 Gb/s NRZ signals at modes $m = 3, 5$ and 7 $(240$, 395 and 550 GHz), of -10 dB intensity, while injecting a HB at zero detuning with an intensity of 0 dB. (a), (b) and (c) Eye diagrams of the converted signals at modes $m = -3, -5$ and -7, denoted as CH1, CH2 and CH3, respectively. Their maximum intensities are: -18 dB, -23 dB and -28 dB. (d), (e) and (f) Eye diagrams of the converted signals when the negated signals are also injected in the counter-propagating direction respect the HB. Their maximum intensities are: -19 dB, -24 dB and -30 dB.

when injecting the incoming signals in the same direction of the HB only . The variations of the high-level are substantially reduced and the eye diagrams largely improved when the negated signals are injected counter-propagating to the HB (see Fig. 5(d-f)). The technical challenges for the practical implementation of this scheme are enormous, and have to be balanced against the improvement achieved in Bit-Error Rate.

4 Conclusion

We have theoretically shown using a realistic TWM that SRLs can perform all-optical simultaneous wavelength conversion of multiple channels by FWM. The model has been validated against experimental data for cavity-enhanced FWM in SRLs [7], and one signal wavelength conversion and multicast [9]. We have extended these approaches for achieving simultaneous multi-channel conversion, paying special attention to cross-talk effects and possible mitigation strategies. Cross-talk between signals arises from the peculiar FWM cascade of modes in SRLs and their cross-gain saturation. Counter-propagating injection of the negated signals allows for substantial reduction of the cross-talk, although its practical implementation seems difficult, hence and a compromise between the quality and the intensities of the converted signals has to be found by adjusting the intensity of the HB, the bias current of the laser and the number, intensity and wavelength of signals that one wants to convert.

These results evidence that SRL-based converters are an interesting alternative to SOA-based converters for moderate bit rates due to their high FWM efficiency, high integrability and low power consumption. Moreover, as in the case of SOAs, we expect that the performance of SRL-based converter can strongly benefit from the use of a quantum dot active medium.

References

[1] G. Contestabile, N. Calabretta, M. Presi, and E. Ciaramella, “Single and multicast wavelength conversion at 40 Gb/s by means of fast nonlinear polarization switching in an SOA,” *IEEE Photon. Technol. Lett.*, vol. 17, no. 12, pp. 2652–2654, Dec. 2005.

[2] C. M. Gallep, H. J. S. Dorren, and O. Raz, “Four-wave-mixing-based dual-wavelength conversion in a semiconductor optical amplifier,” *IEEE Photon. Technol. Lett.*, vol. 22, no. 21, pp. 1550–1552, Nov. 2010.

[3] M. Matsuura, N. Calabretta, O. Raz, and H. J. S. Dorren, “Multichannel wavelength conversion of 50-Gbit/s NRZ-DQPSK signals using a quantum-dot semiconductor optical amplifier,” *Opt. Express*, vol. 19, no. 26, pp. B560–B566, Dec. 2011.

[4] M. T. Hill *et al.*, “A fast low-power optical memory based on coupled micro-ring lasers,” *Nature*, vol. 432, no. 7014, pp. 206–209, Nov. 2004.

[5] K. Thakulsukanant *et al.*, “All-optical label swapping using bistable semiconductor ring laser in an optical switching node,” *J. Lightwave Techn.*, vol. 27, no. 6, pp. 631–638, Mar. 2009.

[6] M. Sorel, P. J. R. Laybourn, G. Giuliani, and S. Donati, “Unidirectional bistability in semiconductor waveguide ring lasers,” *Appl. Phys. Lett.*, vol. 80, no. 17, pp. 3051–3053, Apr. 2002.

[7] S. Fürst and M. Sorel, “Cavity-enhanced four-wave mixing in semiconductor ring lasers,” *IEEE Photon. Technol. Lett.*, vol. 20, no. 5, pp. 366 –368, Mar. 2008.

[8] B. Li *et al.*, “All-optical digital logic and and XOR gates using four-wave-mixing in monolithically integrated semiconductor ring lasers,” *Electron. Lett.*, vol. 45, no. 13, pp. 698 –700, 18 2009.

[9] D. Lu *et al.*, “Configurable all-optical multicast using cavity-enhanced four wave mixing in semiconductor ring laser,” *Electron. Lett.*, vol. 44, no. 23, pp. 1374 –1376, 6 2008.

[10] J. Javaloyes and S. Balle, “Emission directionality of semiconductor ring lasers: A traveling-wave description,” *IEEE J. Quantum Electron.*, vol. 45, no. 5, pp. 431 –438, May 2009.

[11] S. Balle, “Simple analytical approximations for the gain and refractive index spectra in quantum-well lasers,” *Phys. Rev. A*, vol. 57, no. 2, pp. 1304–1312, Feb. 1998.

[12] J. Javaloyes and S. Balle, “Quasiequilibrium time-domain susceptibility of semiconductor quantum wells,” *Phys. Rev. A*, vol. 81, no. 6, p. 062505, Jun. 2010.

[13] ——, “Multimode dynamics in bidirectional laser cavities by folding space into time delay,” *Opt. Express*, vol. 20, no. 8, pp. 8496–8502, Apr. 2012.

[14] L. Gelens *et al.*, “Optical injection in semiconductor ring lasers: backfire dynamics,” *Opt. Express*, vol. 16, no. 15, pp. 10968–10974, Jul. 2008.